BJET
(Bayero Journal of Engineering and Technology)
https://bjet.ng/index.php/jet

Research Article
2026, Vol. 21 (2), 104-110

TRANSIENT STABILITY ENHANCEMENT AND POWER OSCILLATION DAMPING IN A SMIB SYSTEM USING A DUAL LEAD-LAG CONTROLLED TCSC.

L. I. Nasir[1], H. M. Sadiq[2], M. B. Jibril[3]

[1]Federal Polytechnic Daura, Katsina, Nigeria.
[2]Kogi State Polytechnic Lokoja, Nigeria.
[3]Federal Polytechnic Daura, Katsina, Nigeria.

nsrlabaran@gmail.com

Received: 30-04-2026
Revised: 03-07-2026
Accepted: 04-07-2026
Published: 08-07-2026

Abstract: *This paper investigates the transient stability enhancement in a Single Machine Infinite Bus (SMIB) system using a Thyristor Controlled Series Capacitor (TCSC) with a dual lead-lag Power Oscillation Damping (POD) controller. The dynamic model of the SMIB system was subjected to a three-phase fault disturbance. Three operating conditions were considered: without TCSC, with fixed TCSC compensation, and with TCSC and a dual lead-lag POD controller. The controller was designed to improve damping of electromechanical oscillations through phase compensation and gain tuning. The simulations were carried out in a Python-based environment using the SciPy and NumPy libraries. The system dynamics were solved using the solve_ivp numerical integrator with a Runge-Kutta (RK45) method and plots were generated using Matplotlib. The results show that fixed TCSC compensation improves synchronizing performance but does not adequately damp oscillations, whereas the proposed dual lead–lag POD controller reduces peak speed deviation, lowers overshoot, and restores stable operation with a settling time of about 4.2 s.*

Key words: Dual Lead-Lag; FACTS; POD; SMIB; TCSC.

1 Introduction

The expansion of modern power grids has led to increased operation near stability limits (Machowski, Bialek and Bumby, 2011). The Thyristor Controlled Series Capacitor (TCSC), a key Flexible AC Transmission Systems (FACTS) device, offers a rapid means of modulating line reactance (Hingorani and Gyugyi, 2000). To maximize its utility, an active damping signal must be superimposed on the firing angle (Kundur, 1994; (Hingorani and Gyugyi, 2000). The TCSC is a critical member of the FACTS family, increasingly utilized in modern power systems characterized by long transmission lines (Hingorani and Gyugyi, 2000; IEEE, 2016). As established in literature, the TCSC is employed for a wide range of operational roles, including scheduling power flow, reducing net losses, providing voltage support, and limiting short-circuit currents (Mathur and Verma, 2002). Furthermore, its ability to mitigate Sub-Synchronous Resonance (SSR) and provide Power Oscillation Damping (POD) makes it indispensable for enhancing the transient stability of the grid under contingency conditions (Kundur, 1994; IEEE, 2016).

Due to rising environmental and economic constraints, maximizing existing transmission capacity is essential. Integrating a TCSC optimizes system performance by accurately modulating line reactance (Kumkratug, 2012).

Several studies have demonstrated the effectiveness of FACTS-based controllers in improving system stability. Research provided a systematic procedure for the optimal tuning of TCSC parameters in Single Machine Infinite Bus (SMIB) systems, involving rotor speed deviation as the primary objective function for damping (Panda, Padhy and Patel, 2007). Another study on Transient stability in SMIB systems using a TCSC-based controller and Fourth Order Runge-Kutta method, the results indicated that TCSC integration significantly outperforms traditional PSS during symmetrical three-phase faults (Maithil, 2010). A study established that utilizing an exact transmission model that accounts for resistance allows the TCSC to effectively expand the system's decelerating area as defined by the Equal Area Criterion (Del Rosso, Canizares and Doña, 2003). A study addressed control design for both transient and steady-state stability, emphasizing the importance of locally measurable input signals to mitigate adverse control interactions (Agrawal, 2016). Another study explored Fuzzy Based PSS and UPFC devices, noting that while PSS is effective for low-frequency oscillations, FACTS-based designs provide superior active and reactive power regulation (Gandhi, 2013).

Despite the extensive application of FACTS devices for transient stability enhancement, existing TCSC-based approaches largely rely on fixed compensation or single-stage damping controllers, which are insufficient for effective suppression of low-frequency oscillations under severe disturbances. Furthermore, the coordinated interaction between TCSC-based compensation and multi-stage damping controllers, particularly under nonlinear operating conditions and saturation constraints, remains inadequately explored.

Motivated by these limitations, this study investigates the enhancement of transient stability in a SMIB system using a TCSC integrated with a dual lead–lag Power Oscillation Damping (POD) controller. A structured comparative analysis is conducted under uncompensated, fixed-compensation, and actively controlled conditions to evaluate system performance under a severe three-phase fault. The study further distinguishes between the synchronizing contribution of TCSC compensation and the damping effect introduced by the proposed controller, providing deeper insight into coordinated stability improvement.

2 Methodology

2.1 SMIB System Modeling

The non-linear dynamic behavior of the SMIB system is described using the classical swing equations (Kundur, 1994; Saadat, 1999):

$$\frac{d\delta}{dt} = \omega - \omega_s \qquad (1)$$

$$\frac{d\omega}{dt} = \frac{\omega_s}{2H}(P_m - P_e - D\,\frac{\omega-\omega_s}{\omega_s}) \qquad (2)$$

where δ is the rotor angle, ω is the rotor speed, ω_s is the synchronous speed, H is the inertia constant, D is the damping coefficient, P_m and P_e are the mechanical input power and electrical output power respectively.

The electrical power transferred to the infinite bus is given by:

$$P_e = \frac{EV}{X_{eff}} sin\delta \qquad (3)$$

where $P_e$is the electrical output power, E is the generator internal voltage, V is the infinite bus voltage, $X_{eff}$is the effective transmission line reactance including TCSC compensation, and δ is the rotor angle between the generator internal voltage and the infinite bus voltage.

The initial operating condition is determined from the steady-state relationship $P_m = P_e$, ensuring equilibrium prior to disturbance. To simulate a disturbance, a three-phase fault is modeled by reducing the electrical power to 20% of its pre-fault value during the interval t=1.0s to 1.3 s:

$$P_e = 0.2\,.\frac{EV}{X_{eff}} sin\delta \qquad (4)$$

This approach represents a severe but non-zero fault condition, ensuring realistic system stress without immediate numerical instability.

The SMIB parameters were selected based on standard benchmark values used in transient stability studies. The inertia constant H=5 represents a typical generator, while P_m=0.8 p.u. ensures operation near the stability limit. The line reactance X_L=0.9 p.u. reflects a moderately loaded system. Nominal voltage conditions V=1.0 p.u. and E=1.2 p.u. were adopted, with system frequency set at 50 Hz. The base firing angle α_0 =160° ensures TCSC operation in the capacitive region for effective compensation (Kundur, 1994; (Saadat, 1999; Hingorani and Gyugyi, 2000).

The system parameters used in this study are summarized in Table I.

Table I: SMIB System Parameters

Parameter	Symbol	Value (pu)
Generator Inertia	*H*	5
Mechanical Power	*Pm*	0.8
Line Reactance	X_L	0.9
Frequency	*F*	50 Hz
Infinite Bus Voltage	V	1.0
Internal Generator Voltage	E	1.2
Base Firing Angle	α_0	160°

2.2 TCSC Modeling and POD Design

The TCSC is modeled as a variable reactance inserted in series with the transmission line. The effective reactance is defined as (Mathur and Verma, 2002; Panda, Padhy and Patel, 2007; Gandhi, 2013):

$$X_{eff} = X_{line} - X_{tcsc} \quad (6)$$

where X_{tcsc} represents the controllable compensation reactance.

To enhance damping performance, a POD controller based on a dual lead–lag compensator is employed. The controller utilizes rotor speed deviation as the input signal to generate a supplementary control signal.

2.2.1 Washout Filter

A washout filter is used to eliminate steady-state components while allowing oscillatory signals associated with electromechanical dynamics to pass. Mathematically, it is represented as:

$$G_{wash}(s) = \frac{sT_w}{1+ sT_w} \quad (7)$$

where $G_{wash}(s)$denotes the washout filter transfer function, $s$is the Laplace operator, and $T_w$is the washout time constant.

The time constant T_w preserve oscillations within the frequency range of 0.1–2.0 Hz.

2.2.2 Dual Lead-lag Compensator

To compensate for phase lag introduced by the system dynamics and control devices, a dual-stage lead–lag compensator is implemented. A single stage is given by:

$$G_{comp}(s) = \frac{1+sT_{lead}}{1+ sT_{lag}} \quad (8)$$

where $G_{comp}(s)$is the transfer function of the lead–lag compensator, s is the Laplace operator, $T_{lead}$is the lead time constant, and $T_{lag}$is the lag time constant.

The cascaded dual-stage structure is expressed as:

$$G_{ll}(s) = \left(\frac{1+sT_1}{1+ sT_2}\right).\left(\frac{1+sT_3}{1+ sT_4}\right) \quad (9)$$

This configuration provides adequate phase compensation to align the control signal with rotor oscillations for effective damping.

2.2.3 POD Controller and Control Architecture

The complete POD controller transfer function is given by:

$$U_{pod}(s) = K_{pod}\left(\frac{sT_w}{1+ sT_w}\right).\left(\frac{1+sT_1}{1+ sT_2}\right).\left(\frac{1+sT_3}{1+ sT_4}\right) \quad (10)$$

BJET, 2026, Vol. 201(2), 104-110

where K_{pod} is the controller gain and T_1–T_4 are the lead–lag time constants selected to achieve the desired phase compensation.

The TCSC reactance is given as:

$$X_{tcsc} = X_{fixed} + U_{pod} \quad (11)$$

To ensure practical and stable operation, the controller output is constrained within predefined limits:

$$U_{min} \leq U_{pod} \leq U_{max}$$

The overall control structure of the SMIB system incorporating the TCSC and dual lead–lag POD controller is shown in Fig. 1.

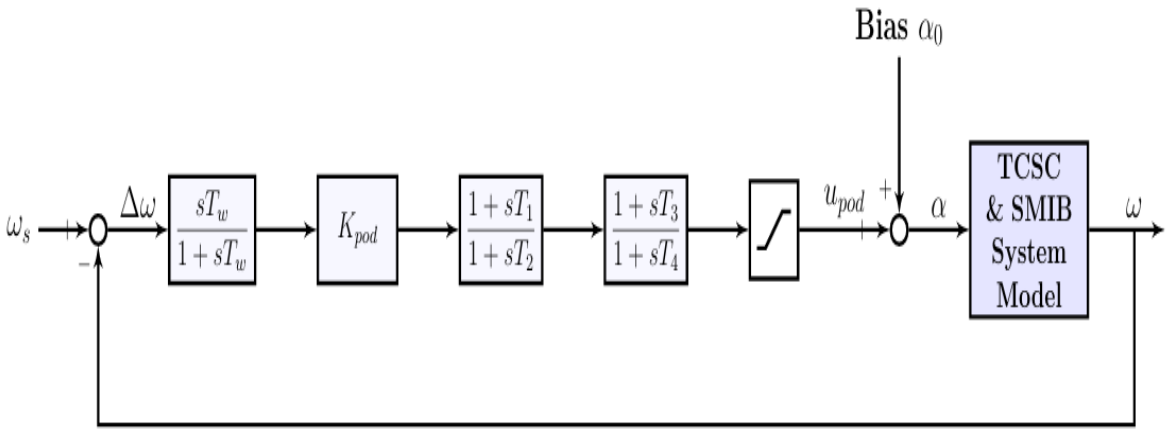

Figure 1: Block Diagram of the SMIB System with Dual Lead-Lag TCSC-Based POD Controller

The dual lead–lag POD parameters were selected based on standard stabilizer design and refined through iterative simulation-based tuning. The gain K_{pod} =20 provides sufficient damping without instability (Kundur, 1994). The washout constant T_w=10 ensures response to transient oscillations while rejecting steady-state components (IEEE, 2016). The lead–lag pairs (T_1, T_2) and (T_3, T_4) = (0.1, 0.05) provide the necessary phase lead (T_{lead}>T_{lag}) for effective damping across electromechanical modes (Mathur and Verma, 2002). The controller output is limited to [-0.15, 0.15] p.u. to maintain practical TCSC operation and avoid overcompensation (Hingorani and Gyugyi, 2000)

The optimized controller parameters used in this study are presented in Table II.

Table II: POD Controller Parameters

Block	Parameter	Value
Gain	K_{pod}	20
Washout Time Constant	T_w	10
Lead Time Constant	T_1 T_3	0.1
Lag Time Constant	T_2 T_4	0.05
Saturation Limts	U_{min}, U_{max}	-0.15, 0.15

2.3. Simulation Setup and Implementation

The nonlinear system equations were solved numerically using the solve_ivp integrator from the SciPy library, employing an explicit Runge–Kutta (RK45) method over a simulation interval of 0–8 s. The solution was evaluated at 1200 uniformly spaced points, corresponding to an approximate sampling interval of 6.7ms. Default solver tolerances were used (relative tolerance 10^{-3}, absolute tolerance 10^{-6}).

The initial rotor angle was obtained from the steady-state power balance condition and slightly perturbed as:

$$\delta_0 = sin^{-1}\left(\frac{P_m X_{line}}{EV}\right) + 0.03 \quad (12)$$

The added perturbation ensures excitation of the electromechanical modes, which is necessary for evaluating the dynamic response of the system. Without this disturbance, the system would remain at equilibrium and no oscillatory behavior would be observed.

Similarly, the initial rotor speed was set to ω_0=1.005 ω_s, representing a small deviation (0.5%) from synchronous speed. This perturbation reflects realistic operating conditions and enables the assessment of damping performance under slight frequency deviations.

A symmetrical three-phase fault was applied between t=1.0s and t=1.3 s. During the fault period, the electrical power transfer capability was reduced to 20% of its nominal value, while pre-fault and post-fault conditions followed the standard power-angle relationship. This approach models a severe but non-zero disturbance, ensuring meaningful transient dynamics without immediate system collapse.

The firing angle alpha (α) was not directly used within the system equations. Instead, it is modulated dynamically based on the POD output using the linear mapping $\alpha = \alpha_{bias} - (U_{pod} \times 60)$, where the base firing angle α_{bias} is 160° and 60 is a scaling factor.

Three operating scenarios are considered for performance evaluation:

- Uncompensated system (Without TCSC)
- Fixed TCSC compensation (With TCSC Only)
- TCSC with dual lead–lag POD controller (With TCSC and POD)

3 Result and Discussion

The transient stability of the SMIB system was analyzed under three operating conditions; without TCSC, with fixed TCSC compensation, and with TCSC coupled with a dual lead-lag POD controller following a three-phase fault applied at t=1.0 s. The dynamic response of the system is assessed using electrical power (Pe), firing angle (α), and rotor speed deviation (Δω) as key performance indicators.

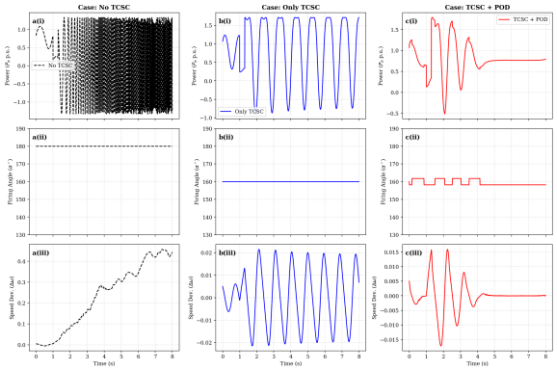

Figure 2: Illustrates the transient behavior of the SMIB system under a three-phase fault for the three operating conditions. (a) Without TCSC: (i) electrical power response, (ii) firing angle, and (iii) rotor speed deviation. (b) With TCSC Only: (i) electrical power response, (ii) firing angle, and (iii) rotor speed deviation. (c) With TCSC and dual lead–lag POD controller: (i) electrical power response, (ii) firing angle, and (iii) rotor speed deviation.

3.1 Case 1: Without TCSC

As shown in Fig. 2a(i), the electrical power exhibits rapidly increasing oscillations following fault clearance, indicating instability in the system. The oscillations grow in both amplitude and frequency, suggesting that the system is unable to regain synchronism. The firing angle in Fig. 2a(ii) remains constant at 180∘, reflecting the absence of any control action. The rotor speed deviation in Fig. 2a(iii) shows a continuous increase over time, confirming divergence from synchronous operation. This behavior clearly indicates loss of synchronism tendency and establishes that the uncompensated system is transiently unstable under the applied disturbance.

3.2 Case 2: With TCSC Only

With fixed TCSC compensation, the electrical power response (Fig. 2b(i)) shows large but bounded oscillations following the fault. Although the amplitude of oscillation is high, it does not diverge as in the uncompensated case. The firing angle in Fig. 2b(ii) remains constant at approximately 160∘, indicating that the TCSC operates at a fixed compensation level without dynamic adjustment. The rotor speed deviation in Fig. 2b(iii) oscillates around zero with sustained amplitude and does not exhibit decay. This confirms that while TCSC improves power transfer capability and prevents instability, it does not introduce sufficient damping to suppress oscillations.

3.3 Case 3: With TCSC and POD

The proposed dual lead-lag POD controller shows a significant improvement in the system performance. The electrical power response in Fig. 2c(i) shows reduced oscillation compared to the fixed TCSC case, with clear damping after fault clearance. The firing angle in Fig. 2c(ii) varies dynamically during the disturbance period, reflecting active control of the TCSC reactance**.** The control signal U_{pod} is constrained by a saturation block to ensure the TCSC operates safely within the Capacitive Vernier region, preventing excessive reactive compensation and ensuring stable operation**.** This enables the controller to respond effectively to system deviations. The rotor speed deviation in Fig. 2c(iii) exhibits a decaying oscillatory response, converging to zero within 4.2 seconds. This indicates that the system successfully regains synchronism and achieves stable operation.

The following table summarizes the key performance metrics extracted from the final simulation results.

Table III: Summary of Performance Metrics

Performance Metric	Without TCSC	With TCSC Only	With TCSC and POD
Transient Stability	Unstable	Underdamped	Stable
Peak Speed Deviation (Δω)	0.450pu	0.022pu	0.016pu
Steady State Power (P_e)	N/A	Oscillatory	0.8pu
Firing Angle Alpha (α)	180 (constant)	160 (constant)	158-162 (Bounded)
Oscillation Overshoot (%)	Unbounded	85%	12%
Settling Time (t_s)	N/A	>8.0s	4.2s
Damping Characteristics	Negative Damping	Sustained Oscillations	Highly Damped

The results in Table III confirm the effectiveness of the proposed controller. The peak speed deviation is reduced from 0.022 p.u. (fixed TCSC) to 0.016 p.u., representing a 27.3% improvement. Similarly, the settling time decreases significantly from beyond 8.0 s to approximately 4.2 s, indicating faster system recovery. The oscillation overshoot is also reduced from about 85% to 12%, confirming substantial enhancement in damping performance. These results demonstrate that while fixed compensation improves synchronizing power, the proposed POD controller provides the necessary damping torque to suppress oscillations and ensure rapid stabilization.

4 Conclusion

This study examined the transient stability of a Single Machine Infinite Bus (SMIB) system using a Thyristor Controlled Series Compensator (TCSC) with a dual lead-lag Power Oscillation Damping (POD) controller under a three-phase fault condition. Simulation results show that the uncompensated system becomes unstable, with increasing rotor speed deviation indicating loss of synchronism. The fixed TCSC improves power transfer but fails to suppress sustained oscillations.

In contrast, the proposed dual lead-lag POD controller provides effective damping, significantly reducing oscillation and restoring system stability within approximately 4.2 seconds after fault clearance. The results demonstrate that the controller introduces sufficient damping torque to mitigate low-frequency oscillations and enhance transient stability. However, the findings are limited to an SMIB model, only one severe disturbance scenario was examined and system performance is sensitive to controller parameters, this sensitivity underscores the necessity for robust optimization techniques, such as Genetic Algorithms or Particle Swarm Optimization, to automate the tuning of T_1–T_4 in varying grid configurations.

References

Agrawal, R., (2016). Transient stability enhancement of SMIB system with fuzzy-based PSS controller and UPFC using MATLAB/Simulink. *International Journal of Advanced Research in Electrical, Electronics and Instrumentation Engineering*, *5*(1).

https://doi.org/10.15662/IJAREEIE.2015.0501018.

Del Rosso, A.D., Canizares, C.A. and Doña, V.M., (2003). A study on TCSC controller design for power system stability improvement. *IEEE Transactions on Power Systems*, *18*(4), pp.1487-1496. https://doi.org/10.1109/TPWRS.2003.818703.

Gandhi, P.K., (2013). Transient stability enhancement of single machine infinite bus system. In: *Proceedings of the 2013 International Conference on Advanced Computing and Communication Systems (ICACCS)*, Coimbatore, India, pp.1-6. https://doi.org/10.1109/ICACCS.2013.6938736.

Hingorani, N.G. and Gyugyi, L., (2000). *Understanding FACTS: Concepts and Technology of Flexible AC Transmission Systems*. New York: IEEE Press.

IEEE, (2016). *IEEE Recommended Practice for Excitation System Models for Power System Stability Studies*. IEEE Std 421.5-2016. Piscataway, NJ: Institute of Electrical and Electronics Engineers.

Kumkratug, P., (2012). The effect of thyristor-controlled series capacitor on transient stability of single machine infinite bus system with the exact short transmission line model. *American Journal of Applied Sciences*, *9*(3), pp.425-428.

Kundur, P., (1994). *Power System Stability and Control*. New York: McGraw-Hill.

Machowski, J., Bialek, J.W. and Bumby, J.R., (2011). *Power System Dynamics: Stability and Control*. 2nd ed. Chichester: John Wiley & Sons.

Maithil, N., (2010). *Transient Stability Enhancement of SMIB System Using TCSC-Based Controller*. B.E. Thesis. Department of Electrical Engineering, National Institute of Technology, Rourkela, India.

Mathur, R.M. and Verma, R.K., (2002). *Thyristor-Based FACTS Controllers for Electrical Transmission Systems*. Piscataway, NJ: IEEE Press.

Panda, S., Padhy, N.P. and Patel, R.N., (2007). Modelling, simulation and optimal tuning of TCSC controller. *International Journal of Simulation Modelling*, *6*(1), pp.37-48.

Saadat, H., (1999). *Power System Analysis*. New York: McGraw-Hill.